Development/Plasticity/Repair

Semaphorin-6D and Plexin-A1 Act in a Non–Cell-Autonomous Manner to Position and Target Retinal Ganglion Cell Axons

Delphine S. Prieur,[1,2,3] Cédric Francius,[1,2,3] Patricia Gaspar,[1,2,3] Carol A. Mason,[5,6] and Alexandra Rebsam[1,2,3,4]

[1]Institut National de la Santé et de la Recherche Médicale, Unité Mixte de Recherche-S 839, Paris, 75005, France, [2]Sorbonne Université, Paris, 75005, France, [3]Institut du Fer à Moulin, Paris, 75005, France, [4]Sorbonne Université, Institut National de la Santé et de la Recherche Médicale, Centre National de la Recherche Scientifique, Institut de la Vision, Paris, F-75012, France, [5]Departments of Pathology and Cell Biology, Neuroscience, and Ophthalmology, College of Physicians and Surgeons, Columbia University, New York, NY 10032, and [6]Mortimer B. Zuckerman Mind Brain Behavior Institute, Columbia University, New York, NY 10027

Semaphorins and Plexins form ligand/receptor pairs that are crucial for a wide range of developmental processes from cell proliferation to axon guidance. The ability of semaphorins to act both as signaling receptors and ligands yields a multitude of responses. Here, we describe a novel role for Semaphorin-6D (Sema6D) and Plexin-A1 in the positioning and targeting of retinogeniculate axons. In *Plexin-A1* or *Sema6D* mutant mice of either sex, the optic tract courses through, rather than along, the border of the dorsal lateral geniculate nucleus (dLGN), and some retinal axons ectopically arborize adjacent and lateral to the optic tract rather than defasciculating and entering the target region. We find that Sema6D and Plexin-A1 act together in a dose-dependent manner, as the number of the ectopic retinal projections is altered in proportion to the level of Sema6D or Plexin-A1 expression. Moreover, using retinal *in utero* electroporation of Sema6D or Plexin-A1 shRNA, we show that Sema6D and Plexin-A1 are both required in retinal ganglion cells for axon positioning and targeting. Strikingly, nonelectroporated retinal ganglion cell axons also mistarget in the tract region, indicating that Sema6D and Plexin-A1 can act non–cell-autonomously, potentially through axon–axon interactions. These data provide novel evidence for a dose-dependent and non–cell-autonomous role for Sema6D and Plexin-A1 in retinal axon organization in the optic tract and dLGN.

Key words: **axon guidance; development; fasciculation; retina; semaphorin; visual system**

Significance Statement

Before innervating their central brain targets, retinal ganglion cell axons fasciculate in the optic tract and then branch and arborize in their target areas. Upon deletion of the guidance molecules Plexin-A1 or Semaphorin-6D, the optic tract becomes disorganized near and extends within the dorsal lateral geniculate nucleus. In addition, some retinal axons form ectopic aggregates within the defasciculated tract. Sema6D and Plexin-A1 act together as a receptor-ligand pair in a dose-dependent manner, and non–cell-autonomously, to produce this developmental aberration. Such a phenotype highlights an underappreciated role for axon guidance molecules in tract cohesion and appropriate defasciculation near, and arborization within, targets.

Received Jan. 10, 2022; revised Apr. 4, 2023; accepted May 1, 2023.

Author contributions: D.S.P., C.F., and A.R. designed research; D.S.P., C.F., and A.R. performed research; D.S.P., C.F., and A.R. analyzed data; D.S.P. wrote the first draft of the paper; D.S.P., C.A.M., and A.R. wrote the paper; D.S.P., C.F., P.G., C.A.M., and A.R. edited the paper.

This work was supported by Institut National de la Santé et de la Recherche Médicale, Sorbonne Université, ANR Grant ANR-12-BSV4-0002, and Retina France Grant to A.R.; LabEx LIFESENSES (ANR-10-LABX-65) and IHU FOReSIGHT (ANR-18-IAHU-01) for the Institut de la Vision, and French Ministry of Education and Research doctoral fellowship to D.S.P.; and National Institutes of Health Grant R01EY012736 to C.A.M. We thank the imaging and animal facilities at the Institut du Fer à Moulin; Stéphane Fouquet (Institut de la Vision) for help for the confocal imaging of the RNAscope experiment; and Takeshi Sakurai and Pierre Godement for valuable input.

The authors declare no competing financial interests.

Correspondence should be addressed to Alexandra Rebsam at alexandra.rebsam@inserm.fr.

https://doi.org/10.1523/JNEUROSCI.0072-22.2023

Introduction

Throughout the brain and spinal cord, afferent axons course as tracts before defasciculating and forming collaterals that enter target regions, branching into synaptic arbors. In the mouse visual system, retinal ganglion cell (RGC) axons from each eye grow toward the optic chiasm, guided ipsilaterally or contralaterally, fasciculate within the optic tract, and then enter their thalamic targets, such as the dLGN (Tuttle et al., 1998; Sitko et al., 2018). Most RGC axons remain at the pial surface of the dLGN as they continue to course toward the midbrain (Godement et al., 1984; Tuttle et al., 1998). To innervate the dLGN, a subset of RGC axons terminating in the superior colliculus, emits a collateral to the dLGN. Retinal axons reach the dLGN around E16 but

do not enter and branch within the dLGN until P0 (Godement et al., 1984). At P3, retinal axon collaterals from both eyes have innervated the dLGN and are intermingled. From P4, retinal axon terminals begin to branch profusely and concomitantly prune exuberant branches (Dhande et al., 2011), leading to the segregation of ipsilateral and contralateral axons in different regions of the dLGN by P7 (Godement et al., 1984; Jaubert-Miazza et al., 2005; Koch et al., 2011; Hong et al., 2019).

Topographic mapping within the dLGN and SC and the role of ephrins and their Eph receptors have been demonstrated (Triplett and Feldheim, 2012), but the molecular mechanisms for prior steps, such as RGC axon tract organization and target entry, are not well understood (Seabrook et al., 2017; Zhang et al., 2017). Evidence suggests that the time a RGC axon arrives in the brain is correlated with its targeting strategy (Osterhout et al., 2014). The few molecules that have been identified include: Cadherin 6 for targeting to the olivary pretectal nuclei (OPN) (Osterhout et al., 2011), Contactin-4 (CNTN4), and amyloid precursor protein (APP) to the nucleus of the optic tract (NOT) (Osterhout et al., 2015), Reelin and its receptor to the ventrolateral lateral geniculate nucleus (vLGN), and intergeniculate leaflet (IGL) (Su et al., 2011). While Semaphorin 6A and PlexinA2/A4 are important for retinal axon targeting to the medial terminal nucleus (MTN) (Sun et al., 2015), in general, Semaphorins and their receptors have been implicated primarily in axon guidance at decision regions, such as the optic chiasm (Sakai and Halloran, 2006; Kuwajima et al., 2012), the floor plate (Zou et al., 2000; Nawabi et al., 2010), and corpus callosum (Niquille et al., 2009; J. Zhou et al., 2013).

Semaphorins can act as attractive or repulsive cues through Plexin and Neuropilin receptors (Kolodkin and Tessier-Lavigne, 2011). As Neuropilins do not seem to have clear transduction capacity, the main functional receptors for Semaphorins are Plexins (Winberg et al., 1998; Tamagnone et al., 1999). In addition, transmembrane Semaphorins can also mediate "reverse" signaling, acting as receptors to initiate downstream signaling cascades (Jongbloets and Pasterkamp, 2014; Battistini and Tamagnone, 2016). In *Drosophila*, Sema-1a is required for axon fasciculation, targeting, and synapse formation involving both forward and reverse signaling (Godenschwege et al., 2002; Cafferty et al., 2006; Komiyama et al., 2007; Yu et al., 2010; Jeong et al., 2012). The closest vertebrate homologs to Sema-1a are the Class 6 Semaphorins, Sema6A–6D (L. Zhou et al., 1997), which are also capable of bidirectional signaling. Semaphorins can signal in *trans* or in *cis* (Jongbloets and Pasterkamp, 2014; Battistini and Tamagnone, 2016), adding complexity to their signaling possibilities.

Here, we identify a new role for Sema6D and Plexin-A1 in RGC organization in the optic tract and entry to the dLGN. In loss of function experiments, we determine that Sema6D and Plexin-A1 interact in a dose-dependent manner for proper organization within the optic tract at the outer limits of the dLGN, proper axonal positioning, fasciculation, and target invasion. We also describe for the first time a non–cell-autonomous effect for both Sema6D and Plexin-A1, suggesting that bidirectional interactions, within and across axons, may mediate the same biological process.

Materials and Methods

Animals. The *Plexin-A1*$^{-/-}$ mouse line (Yoshida et al., 2006) and the *Sema6D*$^{-/-}$ mouse line (Takamatsu et al., 2010) were maintained in a C57BL6 background. *Plexin-A1*$^{-/-}$; *Sema6D*$^{-/-}$ double heterozygotes were generated from these mutants. These mice are born at Mendelian ratios and survive to adulthood. For genotyping of the two mouse lines, mouse tails were immersed in 50 mM NaOH at 95°C for 1 h and then neutralized with 1 M Tris-HCl. PCR was performed on the tail lysates using the following primers: PlxA1 WT forward: 5′-CC TGCAGATTGATGACGACTTCTGC-3′, PlxA1 WT reverse: 5′-TCATGCAGACCCAGTCTCCCTGTCA-3′; PlxA1 mutated forward: 5′-GCATGCCTGTGACACTTGGCTCACT-3′, PlxA1 mutated reverse: 5′-CCATTGCTCAGCGGTGCTGTCCATC-3′; Sema6D forward 5′-ACAAACGAGAAACCAGTTTCACC-3′, Sema6D reverse: 5′-CCAGCAATATAAAGTGTGTCTCG-3′. PlxA1 WT band: 200 bp, PlxA1 mutated band: 600 bp, Sema6D WT band: 850 bp; Sema6D mutated band: 1370 bp.

All animal procedures followed the regulatory guidelines of the Columbia University Institutional Animal Care and Use Committee and were approved (animal protocol #2496) by the French Ministry of Agriculture and Forestry, and conducted in compliance with the European community ethical guidelines (decree 2010/63/UE).

Plasmids. The plasmids used were obtained by cloning using the following vectors and oligonucleotides. For the shRNA plasmids, shRNA was obtained directly in pLKO vector from Sigma. Scrambled shRNAs were designed and corresponding oligonucleotides were integrated in Sigma MISSION pLKO.1-puro Empty Vector Control Plasmid DNA using The RNAi Consortium-Broad Institute protocol. shRNA and the mU6 promoter were then cut and placed in a pCAGGS-dsRed2 vector using T4 DNA-ligase (Extended Data Fig. 4-1).

Anterograde labeling of retinogeniculate projections and perfusion. Ocular injections of fluorescent cholera-toxin subunit B (CTB, Invitrogen) were done as previously described in Rebsam et al. (2009). Briefly, P2 to P6 mice were anesthetized on ice during 5-8 min. P13 mice were anesthetized with ketamine-xylazine (75 and 15 mg/kg) in NaCl 0.9% and concentrations were multiplied by 2 for the adult mice (>1 month). After anesthesia, each eye was injected intravitreally twice (diametrically opposed injections) with a glass micropipette (Drummond) for a total of 2-3 µl of 0.2% CTB (Invitrogen) conjugated to AlexaFluor (AF) 488, 594 or 647 diluted in 1% DMSO (see Fig. 2*K*). AF488 and/or AF594 were used for ocular tracing of mutant mice (see Figs. 1, 2, 4, 5). AF594 and AF647 were used for clearing with iDISCO^{+} protocol as AF488 gives strong background (see Fig. 2*L–O*). AF488 and AF647 were used after electroporation experiments with DsRed2 (see Fig. 4). If eyes were not naturally open (at P3), the skin was cut with a scalpel following the natural line between the two eyelids. Mice were anesthetized with pentobarbital (547 mg/kg) and then perfused transcardially with 4% PFA in 0.12 M PB, 24 h (P3) or 48 h (P15-adult) after tracer injection.

In utero *retinal electroporation. In utero* retinal electroporation was adapted from our previously published method (Petros et al., 2009). Briefly, *in utero* retinal electroporation was done at E14.5 to electroporate a large number of RGCs, as their production peaks at this age (Drager, 1985) and electroporation is most efficient when RGCs are in their last cell division. Pregnant WT mice (Janvier Labs) were anesthetized using isoflurane. Left eyes of E14.5 embryos were injected using a glass micropipette (Drummond) and an INJECT+MATIC Microinjector with a mix of plasmidic DNA generated as described above: pCAGGS-shRNAs-DsRed2 at 2 µg/µl (Extended Data Fig. 4-1). Eyes were then electroporated with 5 pulses of 45 V lasting 50 ms each, every 950 ms (Nepagene electroporator) using CUY650P5 electrodes (Sonidel). For whole eye electroporation, the positive electrode was placed on the injected eye and the negative electrode at the opposite side. This electrode positioning mostly targets RGCs at the center of the retina, sparing ventro-temporally located ipsilateral RGCs. Mice were then injected subcutaneously with flunixin (16 mg/kg) for postsurgery analgesia. To increase the survival of the pups, a Swiss female mated 1 d earlier than the C57BL6 electroporated mice was added to each cage of 2 electroporated mice. After birth of Swiss pups, only 3 Swiss pups were kept to stimulate nursing.

Immunohistochemistry and brain clearing. After perfusion, mice brains were dissected. Brains and rest of the head were postfixed

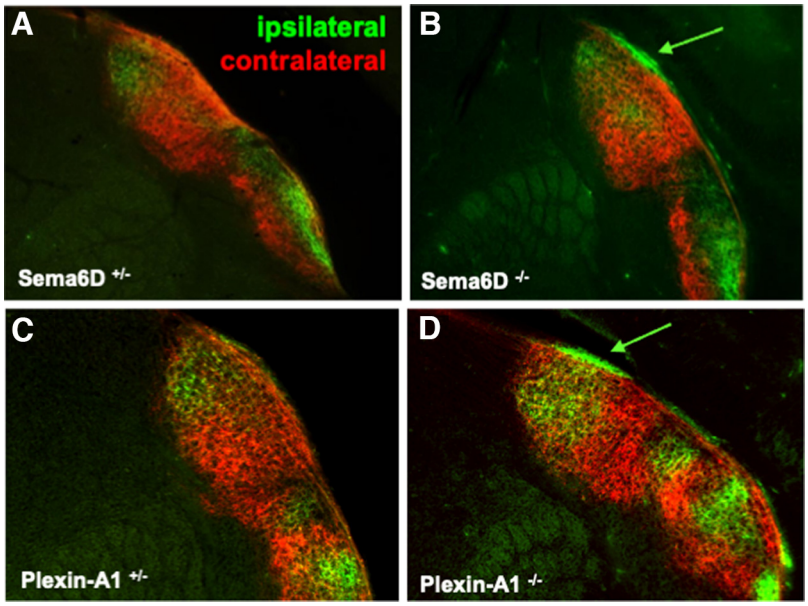

Figure 1. ***A–D***, Sema6D and Plexin-A1 are involved in dLGN targeting by retinal axons during innervation early postnatally. Eye-specific projections to dLGN on coronal slices in heterozygotes (as a control) and mice lacking Plexin-A1 or Sema6D at P3. Ipsilateral (green) and contralateral (red) projections were labeled by ocular injection of CTB, coupled with a fluorophore. The dLGN in *Plexin-A1*$^{-/-}$ and *Sema6D*$^{-/-}$ mice at P3 have ectopic ipsilateral projections (arrows) localized in the lateral aspect of the optic tract, between the optic tract and pia lining the ventricle.

overnight at 4°C in 4% paraformaldehyde in PB 0.12M (PFA). Retinae were then dissected, oriented with an incision in the dorsal part, immunolabeled as described below, and whole-mounted. Brains were cryoprotected in a bath of PBS, 30% sucrose and 0.01% azide sodium during 24 h. CTB-injected brains were then coronally cut at 60 µm with a freezing microtome (Microm). They were immunolabeled and mounted as retinas in moviol-dabco (Calbiochem, Sigma). Electroporated retinae and brain slices were washed in PBS, blocked in 0.1% Triton, 10% horse serum, 0.01% azide sodium in PBS for 30 min, and incubated at 4°C overnight with primary antibodies in blocking solution followed by incubation with secondary antibodies at room temperature for 1 h. In between and after antibody incubations, tissues were washed 3 times 10 min in PBS, 0.1% Triton. For DAPI staining, an additional bath of DAPI diluted at 1/2000 in PBS, 0.1% Triton was added just after secondary antibody incubation.

Some whole P15 brains, labeled with CTB, were dissected (removal of the cortex and separation of the two hemispheres) and cleared following the iDISCO$^+$ protocol without immunostaining (Renier et al., 2016).

In situ hybridization (ISH). After perfusion with 4% PFA in PB 0.12 M, P5 eyes and P7 mice brains were dissected, postfixed overnight at 4°C in 4% PFA, then rinsed in PB 0.12 M. Brains and eyes were cryoprotected overnight in 10% sucrose in PB 0.12 M. Brains were embedded in 7.5% gelatin and 10% sucrose in PB 0.12 M (DIG-ISH) and eyes directly in optimal cutting temperature compound before freezing in cold isopentane (−55°C); 20 µm coronal sections for brains and 16 µm eye sections were cut on a cryostat (Leica) and air dried briefly.

Brain sections were fixed for 10 min in 4% PFA, washed 3 × 3 min in PBS. Proteinase K (5 µg/ml) in PBS for 10 min (or less) was used followed by 3 × 3 min washed in PBS. An acetylation step with TEA was performed for 10 min. Sections were then prehybridized 2 h at 68.5°C in hybridization buffer (50% formamide, 5× SSC, 5× Denhardts, 250 µg/ml *E. coli* tRNA, 500 µg/ml herring sperm), then overnight in hybridization buffer with RNA probe at 68.5°C. After several washes (5× SSC, 0.2× SSC), sections were equilibrated in B1 buffer (0.1 M Tris, pH 7.5; 0.15 M NaCl), incubated in blocking solution (B1 + 10% sheep serum) for 1 h at room temperature and in anti-DIG solution (B1 + 1% sheep serum + 1/5000 anti-DIG-AP antibody) overnight at 4°C. After rinses in B1, sections were equilibrated in B3 (0.1 M Tris, pH 9.5; 0.1 M NaCl; 50 mM $MgCl_2$). Color reaction was performed in B3 solution with 5-bromo-4-chloro-3-indolyl-phosphate (BCIP) (3.5 µl/ml), Nitroblue tetrazolium chloride (NBT) (3.5 µl/ml), and levamisol (0.24 mg/ml) in the dark until staining was observed. The reaction was stopped by rinsing sections in TE pH 8 several times, fixing in PFA 4% for 30 min, washing in PBS. Sections were coverslipped and mounted in Gel Mount.

For fluorescent ISH, sections of the eye were processed according to the manufacturer's protocol described in RNAscope multiplex Fluorescent Reagent kit V2 Assay (BioTechne) for Plexin-A1-C1 and Sema6D-C2 custom-made probes with a few adjustments: target retrieval was done for 5 min at 96°C -100°C, Protease III was applied for 15 min at room temperature. TSA vivid fluorophore kit (Tocris Bioscience) was used for fluorescence signal revelation. Plexin-A1-C1 was revealed with TSA 570 and Sema6D-C2 with TSA 650. Sections were mounted with Prolong Gold Anti-fade (Invitrogen).

Imaging. Whole-mount retinae and brains were imaged using a Leica-DM6000 fluorescence microscope with a 10×/0.3 objective, and the complete image of the retina was reconstructed with MetaMorph software. CTB-labeled brains were imaged with a 10×/0.4 objective. The high-resolution images of ectopic aggregates and electroporated axons in dLGN were obtained by *z*-stack projection of images using a Leica SP5 confocal microscope and a 40× objective. Dissected brains cleared by the iDISCO$^+$ method (Renier et al., 2016) were imaged using a Leica SP5 confocal microscope and a 10× objective. Sections processed for RNAscope were imaged using an Olympus FV3000 laser-scanning confocal microscope equipped with high-sensitivity GaAsP detectors using Olympus Fluoview software FV31S Version 2.61.243. The objective used was an Olympus UPLXAPO20X NA 0.8 WD 0.6. Exposure settings that minimized oversaturated pixels in the final images were used.

Analysis. The proportion of dLGN occupied by ipsilateral axons was measured as a ratio of ipsilateral pixels to the total number of pixels in the dLGN region (mean percentage ± SEM) and obtained as described in Rebsam et al. (2009). Briefly, using MetaMorph software (Molecular Devices), the boundary of the dLGN was outlined, excluding the intrageniculate leaflet, the ventral lateral geniculate nucleus, and the optic tract. The intensity threshold for the ipsilateral projection was chosen when the signal-to-background ratio was at least 1.2 and the area of ipsilateral projection was measured within the boundary of the dLGN. Statistical analyses were performed using ANOVA test and Student's *t* test.

The number of ectopic aggregates of retinal projections in the dLGN were counted in each brain section containing the normal ipsilateral territory divided by the total number of dLGN sections. The bar represents the mean, and dots represent individual values. Statistical analysis was performed by GraphPad Prism, using the Mann–Whitney nonparametric Student's *t* test. Differences were considered statistically significant when $p < 0.05$. 3D images of CTB-labeled and transparent brains were reconstructed using IMARIS software.

Results

Sema6D and Plexin-A1 are both crucial for proper RGC axon entry in the dLGN

We had previously shown that a complex of Sema6D, Plexin-A1, and NrCAM is necessary for a proper RGC axon divergence at the optic chiasm, based on our finding that in *Sema6D*-KO and *Plexin-A1/NrCAM*-DKO ipsilateral projections were increased at the level of the optic chiasm (Kuwajima et al., 2012). We set out to determine the role of these molecules further along the visual pathway. To trace RGC axon projections to the dLGN, the major target of retinal axons in the brain, we used ocular injections of

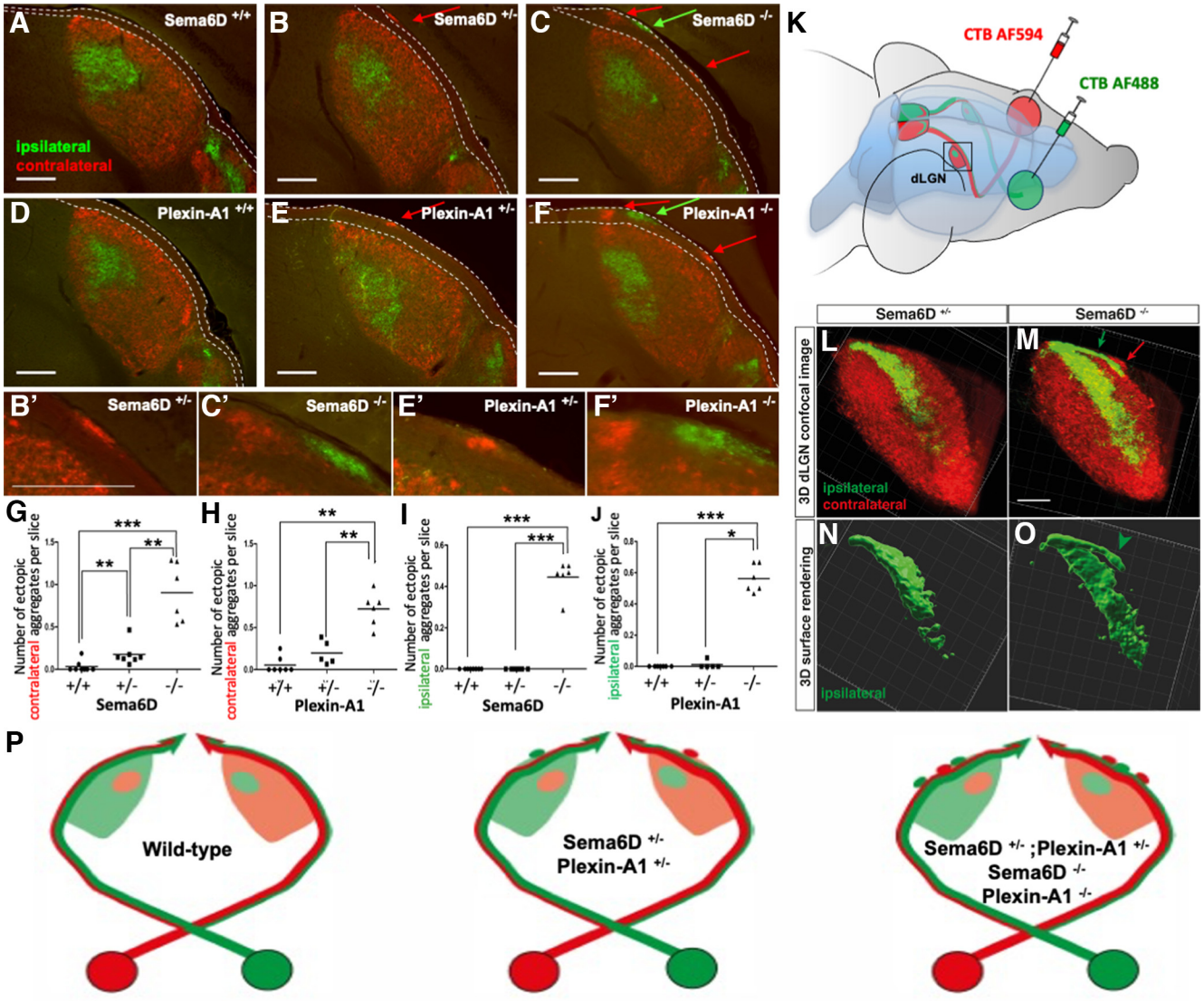

Figure 2. Sema6D and Plexin-A1 are involved in dLGN targeting by retinal axons with a dose-dependent effect. ***A–F***, Eye-specific projections on dLGN coronal slices in WT, heterozygotes, and KO adult mice for Sema6D (***A–C***) and Plexin-A1 (***D,E***). Ipsilateral (green) and contralateral (red) projections were labeled by ocular injection of CTB, coupled with an AlexaFluor dye. In heterozygotes and more prominently in KO mice, the optic tract is entering slightly in the dLGN instead of following it (dashed lines). Compared with WT dLGN, *Plexin-A1*$^{-/-}$ and *Sema6D*$^{-/-}$ dLGNs present some ectopic retinal projections forming aggregates (arrows) localized at the other side of the optic tract, near the ventricle. *Plexin-A1*$^{-/-}$ mice (***F***) and *Sema6D*$^{-/-}$ mice (***C***) show ipsilateral and contralateral ectopic aggregates in slices, whereas *Plexin-A1*$^{+/-}$ (***E***) and *Sema6D*$^{+/-}$ (***B***) present only contralateral ectopic aggregates. ***G–J***, Quantification of the number of ectopic aggregates on each dLGN slice containing ipsilateral projections divided by the total number of dLGN slices. ***K***, Schematic representation of eye-specific injection with CTB-AlexaFluor (CTB AF) 488 and 594 and the retinal projections labeled in the mouse brain. ***L***, ***M***, Ipsilateral ectopic projections in Sema6D mutant mice are an extension of the normal ipsilateral projections. Eye-specific projections in 3D dLGN in *Sema6D*$^{+/-}$ and *Sema6D*$^{-/-}$ mice at P15, after brain clearing using iDISCO^{+} protocol and confocal 3D imaging. Arrows indicate ectopic projections. ***N***, ***O***, 3D surface rendering of the ipsilateral projection using Imaris software. Arrowhead indicates the ectopic ipsilateral projection that is identified as an isolated aggregate in coronal sections (i.e., Fig. 1*C*) but appears in continuity with the normal ipsilateral projection in 3D. Scale bars: ***A–F***, ***B′–F′***, 200 μm; ***M***, 150 μm. ***P***, Schematic representation of the different phenotypes following deletion of one or both alleles of *Plexin-A1* or/and *Sema6D*. Retinal projections from each eye are labeled in red or green and ectopic projections are represented as aggregates of corresponding colors.

CTB coupled to AlexaFluor dyes, with a different fluorophore in each eye, in P3 mice mutant for *Sema6D* or *Plexin-A1*. In *Sema6D* and *Plexin-A1* mutant mice, striking ectopic ipsilateral projections are positioned external to the normal optic tract at P3 (Fig. 1), at the time when most RGC axons have reached their brain targets, including the dLGN and ipsilateral and contralateral projections overlap within the dLGN. Thus, the increase in ipsilateral projections found at embryonic ages (Kuwajima et al., 2012) is maintained, and these ipsilateral projections are strongly concentrated along the optic tract where most axons have entered and are branching within the dLGN.

When similar ocular injections are done in P15 or adult mice (Fig. 2*K*), the bulk of the projections into the superior colliculus (data not shown) and the dLGN is not affected by the absence of Sema6D or Plexin-A1. The normal ipsilateral core and contralateral shell in the dLGN are maintained, correctly positioned and properly segregated (Fig. 2*A–F*), and no difference is observed in the proportion of dLGN occupied by ipsilateral fibers between all genotypes (*Sema6D*$^{+/+}$:11.2% ± 0.8, *Sema6D*$^{+/-}$: 10.2% ± 0.8, *Sema6D*$^{-/-}$: 9.9% ± 1.2, *Plexin-A1*$^{+/-}$:13.1 ± 1.8, *Plexin-A1*$^{-/-}$: 10.4 ± 1.7). However, although the optic tract normally encompasses the dLGN and runs beneath the pial surface (Fig. 2*A*,*D*), in both single-KO mice (*Sema6D*$^{-/-}$ or *Plexin-A1*$^{-/-}$), the optic tract partially passes through the superficial dLGN, resulting in a small portion of the dLGN positioned lateral to the optic tract as seen in coronal sections (Fig. 2*C*,*F*). Furthermore, whereas in

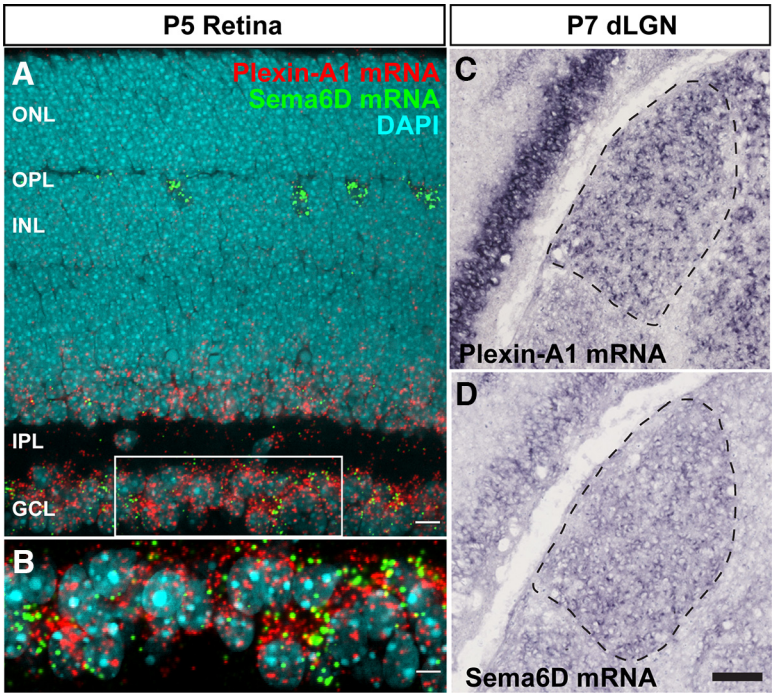

Figure 3. ISH for Sema6D and Plexin-A1 on sections of the retina (***A***,***B***) and coronal sections of the dLGN (***C***,***D***). Both Plexin-A1 and Sema6D are expressed in the retina at P5 and in the dLGN at P7. ***A***, Plexin-A1 is expressed in all cells of the GCL and in most cells of the lower part of the INL. Sema6D is more expressed in a subset of cells in the GCL and in the INL and in a few cells of the upper part of the INL close to the OPL, possibly horizontal cells. ***B***, Higher-magnification image of rectangle in ***B*** confirms that all sema6D-positive cells are also Plexin-A1-positive. A few cells are only Plexin-A1-positive. IPL, Inner plexiform layer; INL, inner nuclear layer; OPL, outer plexiform layer; ONL, outer nuclear layer.

control mice, ipsilateral axons terminate only within the core of the dLGN (Fig. 2*A*,*D*) (Godement et al., 1984; Jaubert-Miazza et al., 2005), in single *Sema6D* or *Plexin-A1* KO mice, some ipsilateral RGCs terminate in small ectopic aggregates in the superficial zone lateral to the displaced optic tract (Fig. 2*C*,*C*′,*F*, *F*′,*I*,*J*). Contralateral axons in single-KO animals also innervate this zone and form ectopic aggregates (Fig. 2*C*,*C*′,*F*,*F*′,*G*,*H*). In contrast, RGC axons in *NrCAM* mutant mice did not display aberrant projections and there was no additional phenotype in *Plexin-A1-NrCAM* DKO compared with *Plexin-A*$^{-/-}$ mice (data not shown). Thus, in *Sema6D*$^{-/-}$ or *Plexin-A1*$^{-/-}$ mice, RGC axons from both eyes form ectopic projections within and superficial to the optic tract that no longer courses around the dLGN cells along the ventricle (Fig. 2*C*,*F*).

Interestingly, heterozygote mice (*Sema6D*$^{+/-}$ or *Plexin-A1*$^{+/-}$) present a similar but milder phenotype to single-KO mice with splaying of the optic tract within the dLGN and contralateral axons forming ectopic aggregates although less extended than in single-KO mice and without any ipsilateral ectopic aggregates (Fig. 2*B*,*E*, *G*–*J*,*P*).

To better describe the aberrant innervation of the dLGN in *Sema6D*$^{+/-}$ and *Sema6D*$^{-/-}$ mouse brains, we used tissue clearing with the iDISCO^{+} technique (Renier et al., 2016). 3D imaging of the labeled retinogeniculate projection in the dLGN showed that the ectopic ipsilateral projections on the outer edge of the optic tract are continuous with the normal ipsilateral projection, forming an ectopic crescent-shaped extension, as a trailing branch along the optic tract in *Sema6D*$^{-/-}$ but not *Sema6D*$^{+/-}$ (Fig. 2*L*–*O*). The ectopic contralateral aggregates are small protrusions from the normal contralateral territory (Fig. 2*M*).

Sema6D and Plexin-A1 are necessary in the retina for proper dLGN targeting in a non–cell-autonomous manner

ISH revealed that Plexin-A1 and Sema6D are both expressed in the ganglion cell layer (GCL) of the mouse postnatal retina as previously described (Fig. 3*A*) (Matsuoka et al., 2011, 2013) and in the dLGN (Fig. 3*C*,*D*). Furthermore, all cells in the GCL, thus all RGCs, express Plexin-A1, while a subset of cells coexpress Sema6D and Plexin-A1.

In order to determine whether Plexin-A1 or Sema6D are necessary in RGCs for the targeting phenotype described above, we electroporated *in utero* at E14.5 shRNA constructs (Extended Data Fig. 4-1) to downregulate Sema6D or Plexin-A1 expression only in the retina. Generally, >25% of the surface of the retina was electroporated (cells labeled with DsRed2 reporter) and almost all electroporated RGCs projected contralaterally as the electroporation targets the center of the retina (Fig. 4*A*–*C*) and ipsilateral RGCs are located in the ventrotemporal retina (Drager and Olsen, 1980). At P13, each eye (electroporated and nonelectroporated) was injected with a different CTB-AlexaFluor dye to trace retinogeniculate projections at P15, once the eye-specific map is mature, to assess whether retinal downregulation of Plexin-A1 or Sema6D is sufficient to perturb retinal projections.

In electroporated mice with retinal knockdown of either Sema6D or Plexin-A1, we observed retinal axon targeting defects in the dLGN with increased branching in the optic tract of electroporated axons (Fig. 4*D*–*F*). Furthermore, in the dLGN located on the side opposite to the eye electroporated with Sema6D or Plexin-A1 shRNA, we observed ectopic contralateral projections (red) next to the optic tract (Fig. 4*D*–*I*). This phenotype is similar to the phenotype observed in *Sema6D*$^{+/-}$ (Fig. 2*B*), *Sema6D*$^{-/-}$ (Fig. 2*C*), *Plexin-A1*$^{+/-}$ (Fig. 2*E*), and *Plexin-A1*$^{-/-}$ mice (Fig. 2*F*). We did not observe ipsilateral aggregates from the electroporated eye possibly because ipsilateral RGCs that are normally located ventrotemporally were not electroporated as our electroporation targets mostly central RGCs (Fig. 4*A*–*C*). While we cannot completely rule out unintended off-target effects, the fact that both deletion of *Plexin-A1* or *Sema6D* in mutant mice and *in utero* retinal knockdown of Plexin-A1 or Sema6D result in a similar, unprecedented phenotype strongly argue for a specific role of these molecules. Thus, this result indicates that Plexin-A1 and Sema6D are both necessary in the retina to properly position RGC axons within the dLGN.

To note, we did not observe any ectopic aggregates in other retinal axon targets, such as the superior colliculus or the vLGN, highlighting the specificity of this phenotype. Importantly, ectopic aggregates on both dLGN sides were mostly composed of axons that were not electroporated with Sema6D or Plexin-A1 shRNA. For instance, the contralateral ectopic aggregates (green) in the outer dLGN found in most cases of Sema6D shRNA electroporation (6 of 8), and a few cases of Plexin-A1 shRNA electroporation (2 of 10) (Fig. 4*N*,*R*), originate from RGCs in the nonelectroporated eye. Similarly, the ipsilateral ectopic aggregates (green) (Fig. 4*H*,*K*) found in half the cases of mice electroporated with Sema6D shRNA correspond to ipsilateral axons

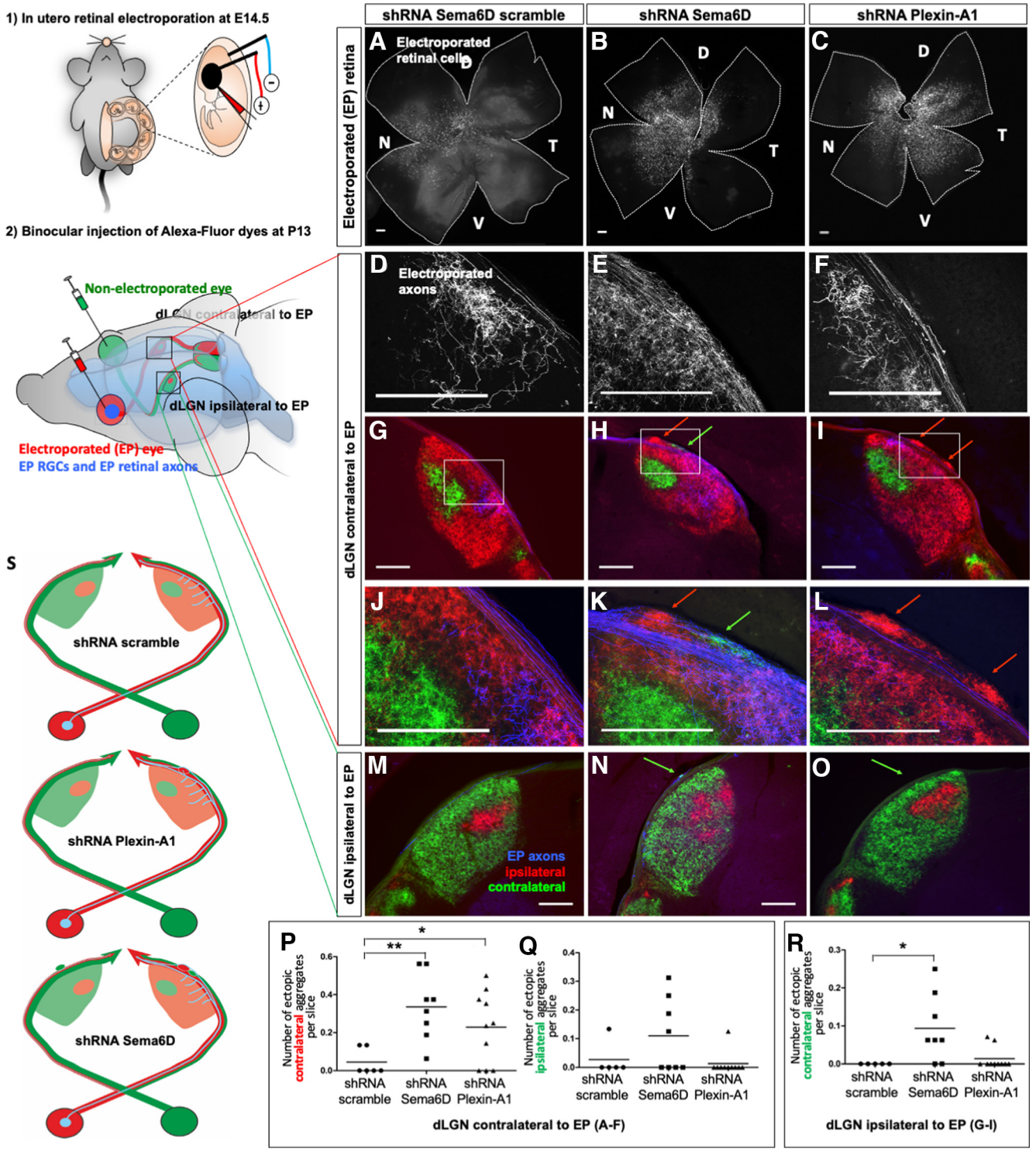

Figure 4. Sema6D and Plexin-A1 act non–cell-autonomously in retinal axons for proper dLGN targeting. ***A–C***, Whole-mount retina at P15 showing electroporated retinal cells (dsred2 reporter) of WT mice after retinal *in utero* electroporation of plasmid coding for shRNAs (Sema6D scramble, Sema6D, or Plexin-A1, see Extended Data Fig. 4-1) at E14.5. ***D–F***, Electroporated retinal axons invading the dLGN contralateral to the electroporated retina. ***G–L***, Eye-specific projections in the dLGN contralateral to the electroporated retina. Ipsilateral (green) and contralateral (red) projections were labeled by ocular injection of CTB, coupled with an AlexaFluor, and electroporated axons (blue) are labeled with the dsred2 reporter. In mice electroporated with Sema6D or Plexin-A1 shRNA, ectopic retinal aggregates (arrows) are located lateral to the optic tract, near the ventricle. ***J–L***, Higher magnification of ***G–I***. Most of the ectopic aggregates are not dsred2-positive, and ipsilateral ectopic aggregates originate from the nonelectroporated eye. ***M–O***, Eye-specific projections in the dLGN ipsilateral to the electroporated retina. Mice electroporated with Sema6D shRNA have contralateral ectopic aggregates (green arrows) originating from the nonelectroporated eye; these ectopic projections form at the lateral edge of the optic tract, and are separated from the pia, similar to the phenotype of the *Plexin-A1* and *Sema6D* KO. Scale bars, 200 μm. ***P–R***, Quantification of the number of ectopic aggregates of each dLGN slice divided by the number of sections containing dLGN. ***S***, Schematic representation of the different phenotypes following knockdown of Plexin-A1 and Sema6D by shRNA. Retinal projections from each eye are labeled in red or green, and electroporated axons are in light blue. The electroporated RGCs (light blue dot) are located in the eye labeled in red.

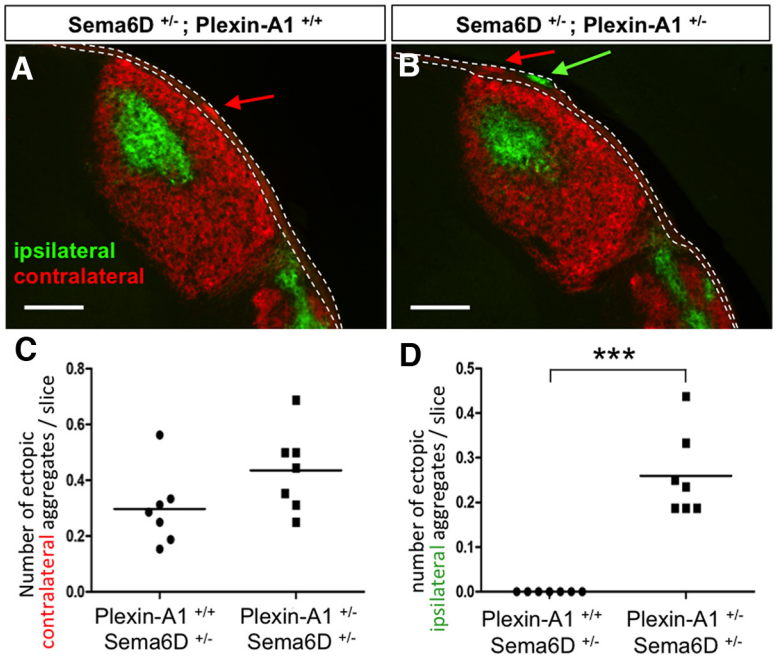

Figure 5. Sema6D and Plexin-A1 act together for proper dLGN targeting by retinal axons. ***A***, ***B***, Eye-specific projections on dLGN coronal slices in simple *Sema6D*$^{+/-}$ heterozygotes and *Sema6D*$^{+/-}$; *Plexin-A1*$^{+/-}$ double heterozygotes at P15. Ipsilateral (green) and contralateral (red) projections were labeled by ocular injection of CTB, coupled with a fluorophore. The phenotype in double heterozygotes is stronger than in simple heterozygotes. *Sema6D*$^{+/-}$; *Plexin-A1*$^{+/-}$ double heterozygotes present some ipsilateral ectopic aggregates, reminiscent of a stronger phenotype specific to the single-*Plexin-A1* or single *Sema6D* KO phenotype. Scale bars: ***C***, ***D***, 200 µm. Quantification of the number of ectopic aggregates of each dLGN divided by the total number of dLGN sections.

arising from the nonelectroporated eye, hence without Sema6D shRNA. Thus, both ipsilateral and contralateral projections from the nonelectroporated eye can form ectopic aggregates (Fig. 4). Moreover, the contralateral ectopic aggregates (red) whose axons do indeed originate from the electroporated eye are composed of only very few DsRed2-positive axons (blue) (Fig. 4*K*,*L*) and mostly nonelectroporated axons. Therefore, a reduction of Plexin-A1 or Sema6D in only a few retinal axons is able to influence the pathfinding and positioning of other retinal axons from the same or opposite eye. This suggests that Plexin-A1 and Sema6D can act non–cell-autonomously for the growth and positioning of retinal axons in the optic tract, potentially through axon–axon interactions.

Sema6D and Plexin-A1 interact for dLGN targeting in a dose-dependent manner

The intermediate phenotype of *Plexin-A1* and *Sema6D* heterozygote mice (Fig. 2*B*,*E*,*P*) suggests that both Plexin-A1 and Sema6D act in a dose-dependent manner for the proper dLGN innervation by retinal axons. As only a total loss of either Plexin-A1 or Sema6D modifies ipsilateral projections (Fig. 2*C*,*F*), this suggests that ipsilateral projections are less sensitive to intermediate levels of Plexin-A1 or Sema6D than the contralateral projections. Sema6D is a Semaphorin that binds the Plexin-A1 receptor (Toyofuku et al., 2004; Yoshida et al., 2006). Furthermore, as both Plexin-A1 and Sema6D KO mice show a similar phenotype concerning retinal projections in the dLGN, it is likely that Sema6D and Plexin-A1 interact together. To identify this putative genetic interaction, we compared retinal projections in the dLGN of *Plexin-A1*$^{+/-}$; *Sema6D*$^{+/-}$ double heterozygotes (Fig. 5*B*) with simple *Sema6D*$^{+/-}$ heterozygotes (Fig. 5*A*). Interestingly, *Plexin-A1*$^{+/-}$; *Sema6D*$^{+/-}$ double heterozygotes display ectopic ipsilateral projections (Fig. 5*B*), a hallmark of the stronger phenotype detected only in *Plexin-A1* or *Sema6D* single-KO (Figs. 2*C*,*F*, 5*E*). Unfortunately, despite breeding efforts, we could not obtain double-KO for Plexin-A1 and Sema6D to assess the effect of the complete loss of both ligand and receptor. Thus, this finding indicates that Plexin-A1 and Sema6D interact together in this newly described aberrant targeting phenotype and supports the notion that Plexin-A1 and Sema6D are indeed a receptor-ligand pair as previously described in this system (Kuwajima et al., 2012) and in the cortico-spinal tract (Yoshida et al., 2006; Gu et al., 2017).

Discussion

Initially discovered as axon guidance molecules, Semaphorins and their receptors have been implicated in cell migration, angiogenesis, bone homeostasis, immune responses, and cancer (Alto and Terman, 2017). Here we show that Plexin-A1 and Sema6D interact for proper retinal axon positioning and cohesion in the optic tract at the surface of the dLGN and entry into this target. Upon downregulation of either Plexin-A1 or Sema6D, or both, in a dose-dependent manner and also on specific downregulation of either molecule in RGCs, the optic tract partially invades the dLGN and some RGC axons form ectopic aggregates laterally to these displaced tract bundles. To our knowledge, such a specific phenotype has not been described previously in any other mutant mouse. Strikingly, we also observed non–cell-autonomous effects: in the electroporation experiments of knockdown of Sema6D or Plexin-A1 in the retina, the ectopic aggregates contained many axons that were not electroporated. This non–cell-autonomous phenotype implies axon–axon interactions involving Sema6D and Plexin-A1. In all, our results show a new role for Plexin-A1 and Sema6D in the developing visual system for the precise targeting of retinal axons at the dLGN.

Plexin-A1/Sema6D participate in different steps of retinal axon development

Recent evidence in *Xenopus* and humans suggests that Plexin-A1 is important for eye development (Cechmanek et al., 2021; Dworschak et al., 2021). However, we did not observe any obvious ocular defects in our Plexin-A1 mutants, and neither molecule appears to be required for retinal lamination or retinal connectivity in the mouse (Matsuoka et al., 2011, 2013). Thus, the phenotype observed in our mutants is not likely because of abnormal retinal development.

Plexin-A1 and Sema6D are a well-known receptor-ligand pair involved in axon guidance at the spinal cord level (Yoshida et al., 2006; Leslie et al., 2011) and at the optic chiasm (Kuwajima et al., 2012), participating in the control of decussation of contralateral retinal axons at the embryonic optic chiasm in a tripartite complex consisting of Plexin-A1, Sema6D, and Nr-CAM (Kuwajima et al., 2012). At the optic chiasm, Nr-CAM and Plexin-A1 convert the repulsive effect of Sema6D on retinal axons into a growth promotion. However, in the present case, Nr-CAM does not seem to be involved in retinal axon positioning and targeting

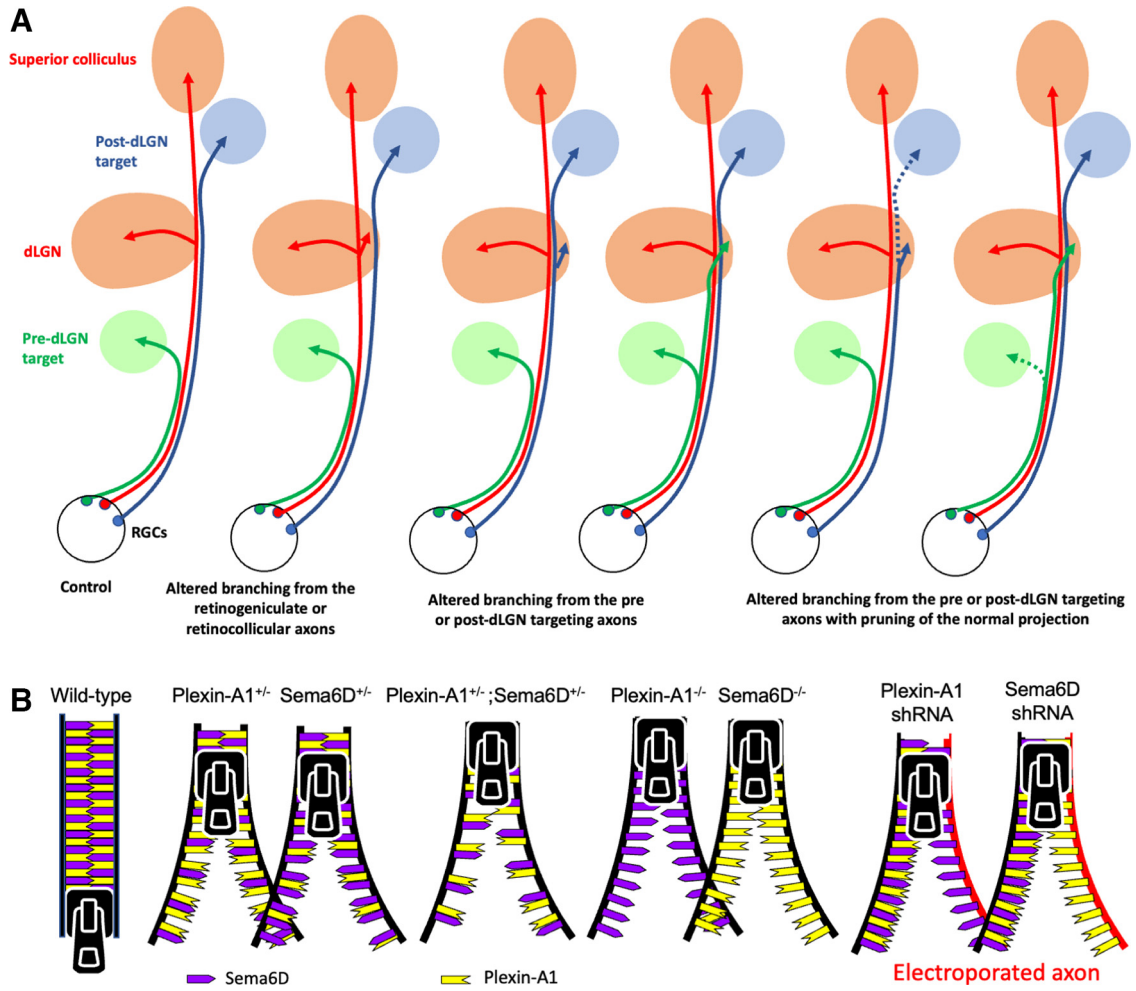

Figure 6. Schematic representations of (***A***) the hypotheses on the axonal origin of ectopic RGC axon aggregates and the defasciculation on altering Sema6D/Plexin-A1 signaling, and (***B***) of a "zipper" model of axon–axon interactions and fasciculation, depending on Plexin-A1 and Sema6D levels and localization. ***A***, The ectopic aggregates could originate either from axons that normally innervate the dLGN or the SC or from axons that normally innervate another target (before or after the dLGN) and either form an additional collateral with or without pruning or the extension of the normal projection into the other target. A combination of all mechanisms could also be possible. ***B***, In this "zipper" model, each side of the zipper represents retinal axons that express both Sema6D and Plexin-A1 and fasciculate together in the optic tract. In WT, the proper ratio and expression level of Sema6D and Plexin-A1 are required for the axons to properly fasciculate and reach the appropriate target, and are represented in a 1:1 ratio and in an alternating arrangement that fits a zipper pattern but may not be the actual distribution or ratio. When Sema6D or Plexin-A1 expression level is reduced (*Plexin-A1*$^{+/-}$, *Sema6D*$^{+/-}$, *Plexin-A1*$^{+/-}$; *Sema6D*$^{+/-}$) or abolished (*Plexin-A1*$^{-/-}$*Sema6D*$^{-/-}$) globally, the proper ratio as well as the strength of the interaction between both sides is altered and the "zipper" malfunctions; thus, axons do not properly fasciculate, and they may branch or innervate ectopic targets, as with the ectopic aggregates in the dLGN. After retinal electroporation of Plexin-A1 or Sema6D shRNA, this downregulation also leads to an altered ratio between both sides and hence to improper fasciculation and ectopic aggregates. The zipper model illustrates the non–cell-autonomous effect described in the text as axons on each side need the optimal ratio and expression levels of both molecules for proper fasciculation of the axons. An alteration even on one side will lead to defasciculation of both the electroporated and nonelectroporated axons.

in the dLGN as *Nr-CAM/Plexin-A1*-DKO have a phenotype similar to that of single *Plexin-A1* KO. Our results are similar to those of Gu et al. (2023), in which deletion of Sema5A/5B-PlexA1/A3 signaling leads to premature defasciculation in the medulla and early termination of CS axons in the cervical rather than lumbar spinal cord.

Our results on *Sema6D* and *Plexin-A1* single KO and double heterozygotes highlight the fact that the same molecules can be reused in the neurons for different steps of axonal development.

While we cannot rule out that other molecules could be important for this phenotype, such as other known ligands of Plexin-A1 (e.g., Sema6C) (Yoshida et al., 2006; Leslie et al., 2011), the similarity in the penetrance and the severity of the phenotype in both *Sema6D* and *Plexin-A1* mutant mice, and the persistence of this phenotype in adult brain (excluding compensatory mechanisms) strongly suggest a direct one-to-one interaction involving only these two molecules.

Plexin-A1/Sema-6D signaling within retinal axons near the dLGN is important for axon positioning

Interestingly, while most retinal axons in WT mice form a cohesive tract and remain at the surface of the dLGN, many retinal axons pass through the dLGN *en route* to other targets (Godement et al., 1984; Jhaveri et al., 1996). Although both types of retinal axons emit small collaterals during early postnatal ages in other rodents, the axons that emit a collateral and arborize within the dLGN represent those coursing in the optic tract at the surface of the dLGN (Bhide and Frost, 1991; Jhaveri et al., 1991). The fact that the optic tract in *Sema6D*$^{-/-}$ or *Plexin-A1*$^{-/-}$ mice courses through the dLGN instead of remaining at the pial surface suggests that certain retinal axons in the mutant mice change their behavior to cues in or around the dLGN and lose their proper positioning. In addition, or alternatively, the aberrant axons may follow retinal axons that pass through the dLGN or cannot follow those that are at the pial surface (Fig. 6*A*). This

phenotype is reminiscent of that observed in the spinal cord where Sema6D and Plexin-A1 signaling controls the axon positioning of proprioceptive sensory axons: proprioceptive axon shafts in *Plexin-A1* or *Sema6D* mutants invade the superficial dorsal horn instead of avoiding this region (Yoshida et al., 2006; Leslie et al., 2011). The ectopic aggregates in our study could be because of the persistence of transient collaterals as seen in cortico-motoneuronal connections of the spinal cord in *Plexin-A1* or *Sema6D* mutants (Gu et al., 2017). However, such a pruning defect is unlikely, as there is no developmental time when the retinal axons arborize so profusely in the dLGN. For instance, at P3, ipsilateral axons are densely branched in the homozygous mutants; but to our knowledge, this does not occur normally during development (Godement et al., 1984; Dhande et al., 2011). Thus, these ectopic aggregates are most likely the result of increased branching or collateral sprouting around retinal axons at the edge of the dLGN rather than within the dLGN. Axon labeling at earlier times would help resolve this issue. It remains to be determined whether the ectopic retinal axons in the dLGN correspond to axons that normally innervate the dLGN or another target and whether in the latter case there is pruning of the normally targeted axons (Fig. 6*A*). Overall, our results suggest that Sema6D/Plexin-A1 signaling is specialized in regulating axon guidance, positioning, and collateral branching across different systems.

Remarkably, although most RGCs that project to the dLGN also project to the SC (Dhande et al., 2011; Ellis et al., 2016), we did not find defects in retinocollicular projections in the mutant mice studied (data not shown). This is surprising as the downregulation of Plexin-A1 or Sema6D in RGCs should affect the entire projection. These positioning and targeting defects highlight specific interactions at the dLGN level rather than general axon–axon interactions all along the path of these retinal axons. One possibility is that a yet unknown molecule on dLGN neurons, glia, or blood vessels could interact with retinal axons for target invasion and branching (Erskine et al., 2017; Clements and Wright, 2018; Lee et al., 2019) and that this interaction would be regulated by the Sema6D/Plexin-A1 signaling. Furthermore, the spatiotemporal sequence of guidance molecules' presence at the axonal membrane could explain a specific role solely near the dLGN as shown for Slits and Semaphorins at the midline of commissural axons for Plexin-A1 (Pignata et al., 2019).

Dose-dependent and non–cell-autonomous effects of both Sema6D and Plexin-A1

A point of interest is that similar effects on retinal axon positioning and targeting are achieved with either Plexin-A1 or Sema6D downregulation in a dose-dependent and non–cell-autonomous manner. Usually, when the ligand is affected, there is a non–cell-autonomous effect of its downregulation; but when the receptor is affected, the effect is cell-autonomous. However, in our case, both act non–cell-autonomously, and Plexin-A1 and Sema6D must thus act in *trans* (in different cells) (Fig. 6*B*). Because Sema6D and Plexin-A1 are expressed together in some RGCs, *cis* interactions (in the same cell) could also be involved (Fig. 6*B*). As semaphorins can act as ligand or receptor, the bidirectional signaling of Sema6D and Plexin-A1 could be important for the regulation of retinal axon positioning and targeting.

The most striking phenotype we observed is that only a few axons electroporated with Sema6D- or Plexin-A1-shRNA can affect the positioning and branching of other nonelectroporated retinal axons coursing with them, regardless of their eye of origin. This suggests an interaction at the level of the optic tract when retinal axons from both eyes converge and specifically near the dLGN considering the localization of the ectopic aggregates only at this location. This consideration reinforces the idea that very few retinal axons, likely those normally expressing Sema6D and Plexin-A1, could be responsible for the mis-positioning and mis-targeting of retinal axons observed in this study.

Here, we propose a "zipper" model of Plexin-A1 and Sema6D interactions to take into account the different phenotypes observed. A normal amount of Sema6D and Plexin-A1 will balance the axon–axon interactions and the axons will fasciculate and form tight bundles in the optic tract (Fig. 6*B*). When Plexin-A1 or Sema6D is reduced in heterozygous mice, this interaction is weakened and axon bundles start to defasciculate and enter the dLGN and ectopic branches/collaterals form (Fig. 6*B*). When Plexin-A1 or Sema6D is absent and when both Plexin-A1 and Sema6D are reduced in double-heterozygotes, axon–axon interactions are further impaired and the phenotype is more severe (Fig. 6*B*). When Sema6D or Plexin-A1 expression is downregulated in a subset of RGCs, the interaction with adjacent nonelectroporated axons will weaken and lead to defasciculation and ectopic branching of both electroporated and adjacent nonelectroporated axons (Fig. 6*B*).

In conclusion, these observations suggest that Plexin-A1 and Sema6D can mediate axon–axon interactions between RGC axons originating from the same or different eyes, and that their interaction is important for retinal axon positioning and targeting.

References

Alto LT, Terman JR (2017) Semaphorins and their signaling mechanisms. Methods Mol Biol 1493:1–25.

Battistini C, Tamagnone L (2016) Transmembrane semaphorins, forward and reverse signaling: have a look both ways. Cell Mol Life Sci 73:1609–1622.

Bhide PG, Frost DO (1991) Stages of growth of hamster retinofugal axons: implications for developing axonal pathways with multiple targets. J Neurosci 11:485–504.

Cafferty P, Yu L, Long H, Rao Y (2006) Semaphorin-1a functions as a guidance receptor in the *Drosophila* visual system. J Neurosci 26:3999–4003.

Cechmanek PB, Hehr CL, McFarlane S (2021) Retinal pigment epithelium and neural retinal progenitors interact via Semaphorin 6D to facilitate optic cup morphogenesis. eNeuro 8:ENEURO.0053-21.2021.

Clements R, Wright KM (2018) Retinal ganglion cell axon sorting at the optic chiasm requires dystroglycan. Dev Biol 442:210–219.

Dhande OS, Hua EW, Guh E, Yeh J, Bhatt S, Zhang Y, Ruthazer ES, Feller MB, Crair MC (2011) Development of single retinofugal axon arbors in normal and beta2 knock-out mice. J Neurosci 31:3384–3399.

Drager UC (1985) Birth dates of retinal ganglion cells giving rise to the crossed and uncrossed optic projections in the mouse. Proc R Soc Lond B Biol Sci 224:57–77.

Drager UC, Olsen JF (1980) Origins of crossed and uncrossed retinal projections in pigmented and albino mice. J Comp Neurol 191:383–412.

Dworschak GC, et al. (2021) Biallelic and monoallelic variants in PLXNA1 are implicated in a novel neurodevelopmental disorder with variable cerebral and eye anomalies. Genet Med 23:1715–1725.

Ellis EM, Gauvain G, Sivyer B, Murphy GJ (2016) Shared and distinct retinal input to the mouse superior colliculus and dorsal lateral geniculate nucleus. J Neurophysiol 116:602–610.

Erskine L, François U, Denti L, Joyce A, Tillo M, Bruce F, Vargesson N, Ruhrberg C (2017) VEGF-A and neuropilin 1 (NRP1) shape axon projections in the developing CNS via dual roles in neurons and blood vessels. Development 144:2504–2516.

Godement P, Salaun J, Imbert M (1984) Prenatal and postnatal development of retinogeniculate and retinocollicular projections in the mouse. J Comp Neurol 230:552–575.

Godenschwege TA, Hu H, Shan-Crofts X, Goodman CS, Murphey RK (2002) Bi-directional signaling by Semaphorin 1a during central synapse formation in *Drosophila*. Nat Neurosci 5:1294–1301.

Gu Z, et al. (2017) Control of species-dependent cortico-motoneuronal connections underlying manual dexterity. Science 357:400–404.
Gu Z, Matsuura K, Letelier A, Basista M, Corey C, Imai F, Yoshida Y (2023) Axon fasciculation, mediated by transmembrane semaphorins, is critical for the establishment of segmental specificity of corticospinal circuits. J Neurosci 43:5753–5768.
Hong YK, Burr EF, Sanes JR, Chen C (2019) Heterogeneity of retinogeniculate axon arbors. Eur J Neurosci 49:948–956.
Jaubert-Miazza L, Green E, Lo FS, Bui K, Mills J, Guido W (2005) Structural and functional composition of the developing retinogeniculate pathway in the mouse. Vis Neurosci 22:661–676.
Jeong S, Juhaszova K, Kolodkin AL (2012) The control of semaphorin-1a-mediated reverse signaling by opposing pebble and RhoGAPp190 functions in *Drosophila*. Neuron 76:721–734.
Jhaveri S, Edwards MA, Schneider GE (1991) Initial stages of retinofugal axon development in the hamster: evidence for two distinct modes of growth. Exp Brain Res 87:371–382.
Jhaveri S, Erzurumlu RS, Schneider GE (1996) The optic tract in embryonic hamsters: fasciculation, defasciculation, and other rearrangements of retinal axons. Vis Neurosci 13:359–374.
Jongbloets BC, Pasterkamp RJ (2014) Semaphorin signalling during development. Development 141:3292–3297.
Koch SM, Dela Cruz CG, Hnasko TS, Edwards RH, Huberman AD, Ullian EM (2011) Pathway-specific genetic attenuation of glutamate release alters select features of competition-based visual circuit refinement. Neuron 71:235–242.
Kolodkin AL, Tessier-Lavigne M (2011) Mechanisms and molecules of neuronal wiring: a primer. Cold Spring Harb Perspect Biol 3:a001727.
Komiyama T, Sweeney LB, Schuldiner O, Garcia KC, Luo L (2007) Graded expression of semaphorin-1a cell-autonomously directs dendritic targeting of olfactory projection neurons. Cell 128:399–410.
Kuwajima T, Yoshida Y, Takegahara N, Petros TJ, Kumanogoh A, Jessell TM, Sakurai T, Mason C (2012) Optic chiasm presentation of Semaphorin6D in the context of Plexin-A1 and Nr-CAM promotes retinal axon midline crossing. Neuron 74:676–690.
Lee H, Scott J, Griffiths H, Self JE, Lotery A (2019) Oral levodopa rescues retinal morphology and visual function in a murine model of human albinism. Pigment Cell Melanoma Res 32:657–671.
Leslie JR, Imai F, Fukuhara K, Takegahara N, Rizvi TA, Friedel RH, Wang F, Kumanogoh A, Yoshida Y (2011) Ectopic myelinating oligodendrocytes in the dorsal spinal cord as a consequence of altered semaphorin 6D signaling inhibit synapse formation. Development 138:4085–4095.
Matsuoka RL, Chivatakarn O, Badea TC, Samuels IS, Cahill H, Katayama K, Kumar SR, Suto F, Chedotal A, Peachey NS, Nathans J, Yoshida Y, Giger RJ, Kolodkin AL (2011) Class 5 transmembrane semaphorins control selective mammalian retinal lamination and function. Neuron 71:460–473.
Matsuoka RL, Sun LO, Katayama K, Yoshida Y, Kolodkin AL (2013) Sema6B, Sema6C, and Sema6D expression and function during mammalian retinal development. PLoS One 8:e63207.
Nawabi H, Briançon-Marjollet A, Clark C, Sanyas I, Takamatsu H, Okuno T, Kumanogoh A, Bozon M, Takeshima K, Yoshida Y, Moret F, Abouzid K, Castellani V (2010) A midline switch of receptor processing regulates commissural axon guidance in vertebrates. Genes Dev 24:396–410.
Niquille M, Garel S, Mann F, Hornung JP, Otsmane B, Chevalley S, Parras C, Guillemot F, Gaspar P, Yanagawa Y, Lebrand C (2009) Transient neuronal populations are required to guide callosal axons: a role for semaphorin 3C. PLoS Biol 7:e1000230.
Osterhout JA, Josten N, Yamada J, Pan F, Wu SW, Nguyen PL, Panagiotakos G, Inoue YU, Egusa SF, Volgyi B, Inoue T, Bloomfield SA, Barres BA, Berson DM, Feldheim DA, Huberman AD (2011) Cadherin-6 mediates axon-target matching in a non-image-forming visual circuit. Neuron 71:632–639.
Osterhout JA, El-Danaf Rana N, Nguyen Phong L, Huberman AD (2014) Birthdate and outgrowth timing predict cellular mechanisms of axon target matching in the developing visual pathway. Cell Rep 8:1006–1017.
Osterhout JA, Stafford BK, Nguyen PL, Yoshihara Y, Huberman AD (2015) Contactin-4 mediates axon-target specificity and functional development of the accessory optic system. Neuron 86:985–999.
Petros TJ, Rebsam A, Mason CA (2009) In utero and ex vivo electroporation for gene expression in mouse retinal ganglion cells. J Vis Exp 31:1333.
Pignata A, Ducuing H, Boubakar L, Gardette T, Kindbeiter K, Bozon M, Tauszig-Delamasure S, Falk J, Thoumine O, Castellani V (2019) A spatiotemporal sequence of sensitization to slits and semaphorins orchestrates commissural axon navigation. Cell Rep 29:347–362.e5.
Rebsam A, Petros TJ, Mason CA (2009) Switching retinogeniculate axon laterality leads to normal targeting but abnormal eye-specific segregation that is activity dependent. J Neurosci 29:14855–14863.
Renier N, Adams EL, Kirst C, Wu Z, Azevedo R, Kohl J, Autry AE, Kadiri L, Umadevi Venkataraju K, Zhou Y, Wang VX, Tang CY, Olsen O, Dulac C, Osten P, Tessier-Lavigne M (2016) Mapping of brain activity by automated volume analysis of immediate early genes. Cell 165:1789–1802.
Sakai JA, Halloran MC (2006) Semaphorin 3d guides laterality of retinal ganglion cell projections in zebrafish. Development 133:1035–1044.
Seabrook TA, Burbridge TJ, Crair MC, Huberman AD (2017) Architecture, function, and assembly of the mouse visual system. Annu Rev Neurosci 40:499–538.
Sitko AA, Kuwajima T, Mason CA (2018) Eye-specific segregation and differential fasciculation of developing retinal ganglion cell axons in the mouse visual pathway. J Comp Neurol 526:1077–1096.
Su J, Haner CV, Imbery TE, Brooks JM, Morhardt DR, Gorse K, Guido W, Fox MA (2011) Reelin is required for class-specific retinogeniculate targeting. J Neurosci 31:575–586.
Sun LO, Brady CM, Cahill H, Al-Khindi T, Sakuta H, Dhande OS, Noda M, Huberman AD, Nathans J, Kolodkin AL (2015) Functional assembly of accessory optic system circuitry critical for compensatory eye movements. Neuron 86:971–984.
Takamatsu H, Takegahara N, Nakagawa Y, Tomura M, Taniguchi M, Friedel RH, Rayburn H, Tessier-Lavigne M, Yoshida Y, Okuno T, Mizui M, Kang S, Nojima S, Tsujimura T, Nakatsuji Y, Katayama I, Toyofuku T, Kikutani H, Kumanogoh A (2010) Semaphorins guide the entry of dendritic cells into the lymphatics by activating myosin II. Nat Immunol 11:594–600.
Tamagnone L, Artigiani S, Chen H, He Z, Ming GI, Song H, Chedotal A, Winberg ML, Goodman CS, Poo M, Tessier-Lavigne M, Comoglio PM (1999) Plexins are a large family of receptors for transmembrane, secreted, and GPI-anchored semaphorins in vertebrates. Cell 99:71–80.
Toyofuku T, Zhang H, Kumanogoh A, Takegahara N, Suto F, Kamei J, Aoki K, Yabuki M, Hori M, Fujisawa H, Kikutani H (2004) Dual roles of Sema6D in cardiac morphogenesis through region-specific association of its receptor, Plexin-A1, with off-track and vascular endothelial growth factor receptor type 2. Genes Dev 18:435–447.
Triplett JW, Feldheim DA (2012) Eph and ephrin signaling in the formation of topographic maps. Semin Cell Dev Biol 23:7–15.
Tuttle R, Braisted JE, Richards LJ, O'Leary DD (1998) Retinal axon guidance by region-specific cues in diencephalon. Development 125:791–801.
Winberg ML, Noordermeer JN, Tamagnone L, Comoglio PM, Spriggs MK, Tessier-Lavigne M, Goodman CS (1998) Plexin A is a neuronal semaphorin receptor that controls axon guidance. Cell 95:903–916.
Yoshida Y, Han B, Mendelsohn M, Jessell TM (2006) PlexinA1 signaling directs the segregation of proprioceptive sensory axons in the developing spinal cord. Neuron 52:775–788.
Yu L, Zhou Y, Cheng S, Rao Y (2010) Plexin a-semaphorin-1a reverse signaling regulates photoreceptor axon guidance in *Drosophila*. J Neurosci 30:12151–12156.
Zhang C, Kolodkin AL, Wong RO, James RE (2017) Establishing wiring specificity in visual system circuits: from the retina to the brain. Annu Rev Neurosci 40:395–424.
Zhou J, Wen Y, She L, Sui YN, Liu L, Richards LJ, Poo MM (2013) Axon position within the corpus callosum determines contralateral cortical projection. Proc Natl Acad Sci USA 110:E2714–E2723.
Zhou L, White FA, Lentz SI, Wright DE, Fisher DA, Snider WD (1997) Cloning and expression of a novel murine semaphorin with structural similarity to insect semaphorin I. Mol Cell Neurosci 9:26–41.
Zou Y, Stoeckli E, Chen H, Tessier-Lavigne M (2000) Squeezing axons out of the gray matter: a role for slit and semaphorin proteins from midline and ventral spinal cord. Cell 102:363–375.